OPEN ACCESS Freely available online

PLoS one

Modeling Retinal Degeneration Using Patient-Specific Induced Pluripotent Stem Cells

Zi-Bing Jin[1,2☯], Satoshi Okamoto[1☯], Fumitaka Osakada[3], Kohei Homma[1], Juthaporn Assawachananont[1], Yasuhiko Hirami[1], Takeshi Iwata[4], Masayo Takahashi[1,5]*

1 Laboratory for Retinal Regeneration, RIKEN Center for Developmental Biology, Kobe, Japan, **2** School of Optometry and Ophthalmology, Eye Hospital, Wenzhou Medical College, Wenzhou, China, **3** Systems Neurobiology Laboratory, The Salk Institute for Biological Studies, La Jolla, California, United States of America, **4** National Institute of Sensory Organs, National Hospital Organization Tokyo Medical Center, Tokyo, Japan, **5** Center for iPS Research and Application, Kyoto University, Kyoto, Japan

Abstract

Retinitis pigmentosa (RP) is the most common inherited human eye disease resulting in night blindness and visual defects. It is well known that the disease is caused by rod photoreceptor degeneration; however, it remains incurable, due to the unavailability of disease-specific human photoreceptor cells for use in mechanistic studies and drug screening. We obtained fibroblast cells from five RP patients with distinct mutations in the *RP1*, *RP9*, *PRPH2* or *RHO* gene, and generated patient-specific induced pluripotent stem (iPS) cells by ectopic expression of four key reprogramming factors. We differentiated the iPS cells into rod photoreceptor cells, which had been lost in the patients, and found that they exhibited suitable immunocytochemical features and electrophysiological properties. Interestingly, the number of the patient-derived rod cells with distinct mutations decreased *in vitro*; cells derived from patients with a specific mutation expressed markers for oxidation or endoplasmic reticulum stress, and exhibited different responses to vitamin E than had been observed in clinical trials. Overall, patient-derived rod cells recapitulated the disease phenotype and expressed markers of cellular stresses. Our results demonstrate that the use of patient-derived iPS cells will help to elucidate the pathogenic mechanisms caused by genetic mutations in RP.

Citation: Jin Z-B, Okamoto S, Osakada F, Homma K, Assawachananont J, et al. (2011) Modeling Retinal Degeneration Using Patient-Specific Induced Pluripotent Stem Cells. PLoS ONE 6(2): e17084. doi:10.1371/journal.pone.0017084

Editor: Mark Mattson, National Institute on Aging Intramural Research Program, United States of America

Received October 28, 2010; **Accepted** January 15, 2011; **Published** February 10, 2011

Funding: This study was supported by the grant from the Ministry of Health, Labour and Welfare, Japan (#H21-Nanchi-Ippan-216). The funders had no role in study design, data collection and analysis, decision to publish, or preparation of the manuscript.

Competing Interests: The authors have declared that no competing interests exist.

* E-mail: mretina@cdb.riken.jp

☯ These authors contributed equally to this work.

Introduction

Retinitis pigmentosa (RP) leads inevitably to visual impairment due to irreversible retinal degeneration, specifically of primary rod photoreceptors. The condition causes night blindness and visual field defects. The disease onset spans a wide range of ages, but RP most often occurs in late life. There is no treatment that allows patients to avoid deterioration of visual function. RP encompasses a number of genetic subtypes, with more than 45 causative genes and a large number of mutations identified thus far. The genetic heterogeneity of RP suggests a diversity of disease mechanisms, which remain largely unclear. Furthermore, for many of the RP subtypes, no appropriate animal models are available. Although large clinical trials have been conducted with α-tocopherol and β-carotene, these studies found no statistically significant change of visual function in RP patients [1,2]. The underlying mutations causing disease in the patients tested in the clinical trials were not revealed, and the variability of individual responses to these drugs is unknown. One of the reasons why these clinical trials failed to examine the effectiveness of drugs is that the effect of a drug may be different between patients with different underlying mutations.

Induced pluripotent stem (iPS) cells reprogrammed from somatic cells [3,4] have enabled us to easily generate patient-derived terminally differentiated cells *in vitro* [5–7]. We have successfully induced differentiation of photoreceptor cells from both human embryonic stem (ES) cells [8] and iPS cells [9,10]. Modeling pathogenesis and treatment *in vitro* using patient iPS cell-derived photoreceptors will elucidate disease mechanisms; circumvent problems related to differences among species that arise when using animal models; decrease patient risk; and reduce the cost of early-stage clinical trials. Here, we generated iPS cells from RP patients with different mutations and demonstrated the potential of patient-derived photoreceptors for disease modeling.

Materials and Methods

RP patients and genetic mutations

The protocol of this study adhered to the tenets of the Declaration of Helsinki. The study was approved by the ethical committees of the Institute of Biomedical Research and Innovation Hospital and the RIKEN Center for Developmental Biology, Japan. Written informed consent from all patients was obtained. We selected five RP patients from four families whose disease-causing mutations have been identified (**Fig. 1A–D and Fig. S1**). Of the five RP patients in this study, three late-onset patients carried the following mutations: 721Lfs722X in *RP1*, W316G in *PRPH2*, and G188R in *RHO*. Two relatively early-onset patients from the same family carried a H137L mutation in *RP9*, which we

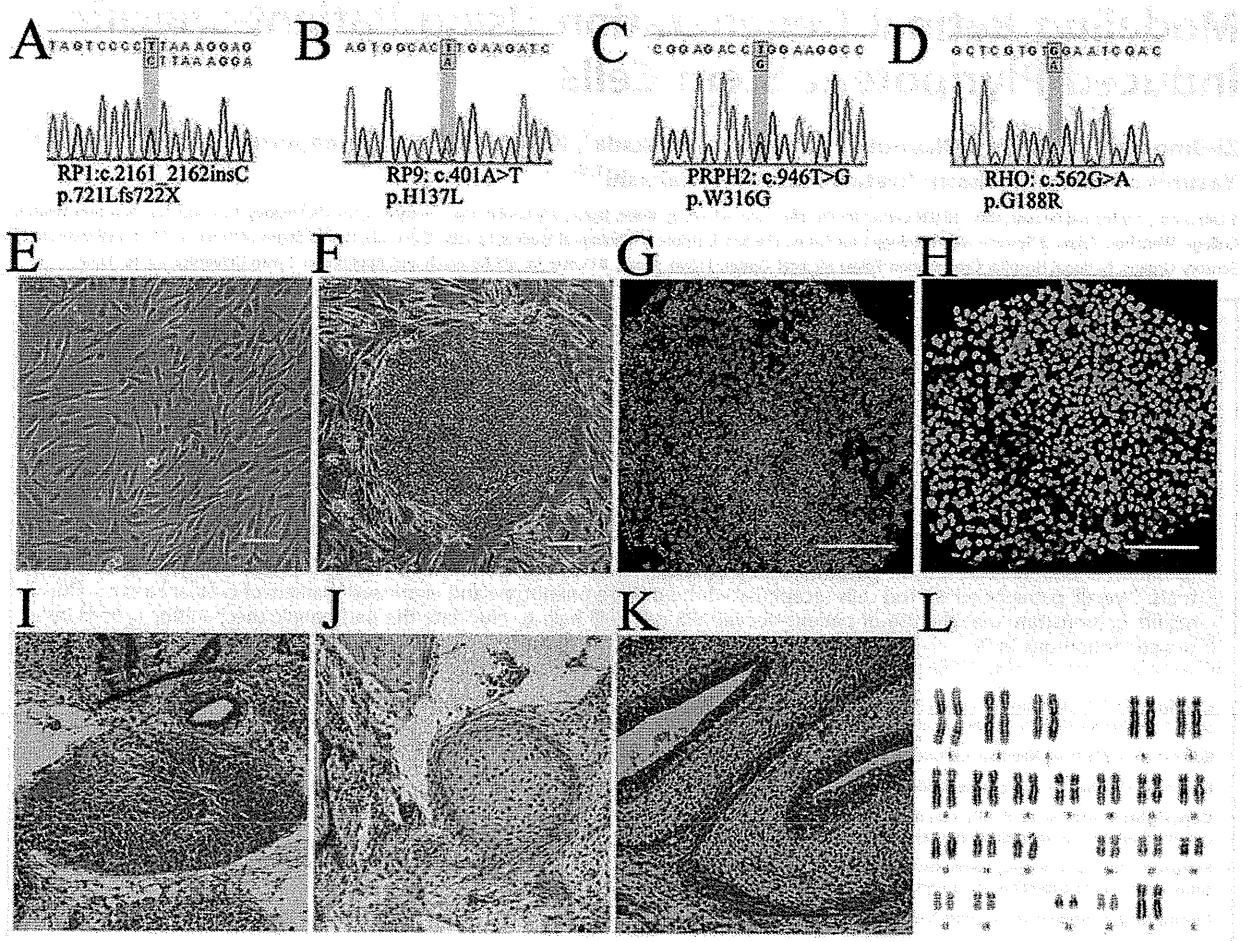

Figure 1. iPS cells derived from RP patients. Mutations identified in patients K21 (RP1) (**A**), K11 and K10 (RP9) (**B**), P101 (PRPH2) (**C**), and P59 (RHO) (**D**). Patient-derived fibroblast cells (**E**) were reprogrammed into iPS cells (**F**). The iPS cells expressed SSEA-4 (**G**) and Nanog (**H**). A teratoma formation test confirmed iPS cells' ability to generate all three germ layers: endoderm (**I**), mesoderm (**J**) and ectoderm (**K**). Karyotype analysis (**I**). Scale bars, 50 μm.
doi:10.1371/journal.pone.0017084.g001

confirmed by both genomic and cDNA sequencing (**Fig. S2**). All patients showed typical manifestations of RP (**Tab. S1**). Peripheral blood obtained from patients was used for DNA isolation. A comprehensive screening of disease-causing genes was carried out as described previously [11]. For the RP9 mutation, total RNA was isolated from fresh blood samples and iPS cells, and synthesized cDNA was subjected to PCR and direct sequencing to confirm whether the mutation was located in the *RP9* gene or the pseudo-RP9 gene (paralogous variant). Both fibroblast and iPS cells were analyzed to re-confirm the identified mutation.

iPS cells generation

To generate iPS cells, retroviral transduction of Oct3/4, Sox2, Klf4, and c-Myc into patient-derived fibroblast cells was carried out as described previously [3]. Established iPS cell lines were maintained on a feeder layer of mitomycin C-treated SNL cells (a murine-derived fibroblast STO cell line expressing the neomycin-resistance gene cassette and LIF) in a humidified atmosphere of 5% CO_2 and 95% air at 37°C. Cells were maintained in DMEM-F12 supplemented with 0.1 mM non-essential amino acids, 0.1 mM 2-mercaptoethanol, 2 mM L-glutamine, 20% KnockOut Serum Replacement (KSR), and 4 ng/ml basic fibroblast growth factor (Upstate Biotechnology).

Transgene quantification

To examine the copy number of transgenes integrated into the host genome, DNA was isolated and quantitative detection of viral transgenes was performed using real-time PCR. The endogenous gene was used as a control. Before quantitative PCR, a standard curve for each primer and/or probe set was determined using a set of plasmid DNA dilutions. Taqman qPCR to detect integrated OCT3/4, KLF4, and MYC was performed using 20 μl reactions consisting of 10 μl TaqMan Master Mix with uracil N-glycosylase, 4.9 μM primers, 250 nM probe, and 1 μl of the DNA sample. Quantification of viral SOX2 was assayed using SYBR Green.

Teratoma formation

Animal protocols were approved by the RIKEN Center for Developmental Biology ethical committee (No. AH18-05). A total of 10^7 trypsinized iPS cells were injected subcapsularly into the testis of SCID mice (two mice per iPS cell line). Four weeks later, the testis was fixed and sectioned for H&E staining.

Immunocytochemistry

Cells were fixed with 4% paraformaldehyde for 15 min at 4°C and then permeabilized with 0.3% Triton X-100 for 45 min. After 1 h blocking with 5% goat serum, cells were incubated with primary antibodies overnight at 4°C and subsequently with secondary antibodies for 1 h at room temperature. The primary and second antibodies used are listed in **Tab. S2**.

Karyotype analysis

Karyotype analysis of the iPS cell chromosomes was carried out using a standard G-band technique (300–400 band level).

Photoreceptor differentiation and drug testing

In vitro differentiation of rod photoreceptor cells was performed as previously reported [8], but with a minor modification. To find a KSR optimal for retinal differentiation, lot testing was conducted before differentiation. iPS colonies were dissociated into clumps with 0.25% trypsin and 0.1 mg/ml collagenase IV in PBS containing 1 mM $CaCl_2$ and 20% KSR. Feeder cells were removed by incubation of the iPS cell suspension on a gelatin-coated dish for 1 h. iPS clumps were moved to a non-adhesive MPC-treated dish (NUNC) in maintenance medium for 3 days, in 20% KSR-containing differentiation medium (DMEM-12 supplemented with 0.1 mM non-essential amino acids, 0.1 mM 2-mercaptoethanol, 2 mM L-glutamine) for 3 days, then in 15% KSR-containing differentiation medium for 9 days, and finally in 10% KSR-containing medium for 6 days. Cells were treated with Lefty-A and Dkk-1 during floating culture. At day 21, the cells were plated en bloc on poly-D-lysine/laminin/fibronectin–coated 8-well culture slides (BD Biocoat) at a density of 15–20 aggregates/cm^2. The cells were cultured in 10% KSR-containing differentiation medium until day 60. Cells were further treated with 100 nM retinoic acid (Sigma) and 100 μM taurine (Sigma) in photoreceptor differentiation medium (GMEM, 5% KSR, 0.1 mM non-essential amino acids, 0.1 mM 2-mercaptoethanol, 1 mM pyruvate, N2 supplement, and 50 units/ml penicillin, 20 μg/ml streptomycin). Differentiated cells from both normal and patient iPS cells were treated with 100 μM α-tocopherol, 200 μM ascorbic acid and 1.6 μM β-carotene starting at differentiation day 120. One week later, cells were fixed for immunostaining.

Electrophysiological recording

Recombinant lentiviral vectors expressing GFP under the control of the Nrl or RHO promoters were generated in HEK293t cells (RIKEN Cell Bank), and differentiated cells were infected with virus on day 90. Cells expressing GFP were targeted for patch clamp recordings. Voltage-clamp recordings were performed with 12–15 MΩ glass electrodes. Signals were amplified using Multiclamp 700B amplifiers (Molecular Devices). The internal solution was 135 mM K-gluconate, 10 mM HEPES, 3 mM KCl, 0.2 mM EGTA, 2.5 mM $MgCl_2$, 5 mM adenosine 5′-triphosphate, 0.3 mM guanosine-5′-triphosphate, 0.06 mM Alexa Fluor 594 (Molecular probes), adjusted to pH 7.6 with KOH. The retinal cells were perfused with oxygen-bubbled external medium: 23 mM $NaHCO_3$, 0.5 mM KH_2PO_4, 120 mM NaCl, 3.1 mM KCl, 6 mM Glucose, 1 mM $MgSO_4$, 2 mM $CaCl_2$, and 0.004% Phenol red. The medium was heated to 37°C with a temperature controller (Warner Instruments).

Cell count and statistical analysis

Differentiated cells visualized with specific antibodies were counted blindly by an independent observer. Data are expressed as means ± s.e.m. The statistical significance of differences was determined by one-way ANOVA followed by Tukey's test or Dunnett's test, or by two-way ANOVA followed by Bonferroni test using the GraphPad Prizm software. Probability values less than 0.05 were considered significant.

Results

Generation of iPS cell lines from patients with RP

Mutations identified in the five patients were confirmed by bi-directional sequencing (**Fig. S1**). Through genotyping of four patients and two normal relatives in the RP9 family, we found the H137L mutation in the *RP9* gene co-segregated with the disease, strongly indicating that the mutation is indeed the genetic cause of the disease. We cultured fibroblasts from skin samples of these patients on gelatin-coated dishes (**Fig. 1E**) and infected them with retroviral vectors encoding *OCT3/4* (also known as *POU5F1*), *SOX2*, *KLF4*, and *c-MYC*, using a previously established method [3]. Each mutation was re-confirmed in both fibroblasts and iPS cells. Established iPS colonies showed human embryonic stem cell-like morphology (**Fig. 1F and Fig. S3A**) and expressed pluripotency markers (**Fig. 1C–D**). We selected iPS cell lines for each patient using multiple criteria. First, we excluded iPS cell lines in which spontaneous differentiation occurred repeatedly during maintenance (**Fig. S3B**). We chose iPS colonies that maintained morphologies similar to those of human ES cells through more than 10 passages. Second, we quantified the transgene copy number and selected iPS cell lines with the fewest integrations, as the risk of gene disruption through random insertion increases with the number of transgenes (**Fig. S4A–E**). Third, in order to select iPS cell lines with full pluripotency, we verified the ability to form teratomas. Teratomas formed by injecting iPS colonies into the testis *in vivo* showed contributions to all three embryonic germ layers: ectoderm, mesoderm, and endoderm (**Fig. 1E–G**). Finally, karyotype analysis was carried out to examine the chromosome integrity. The patient-iPS cells showed normal karyotypes after extended passage, indicating chromosomal stability (**Fig. 1H**). These results provide *in vitro* and *in vivo* functional proof of pluripotency for RP patient-derived iPS cells.

Generation of patient-specific retinal photoreceptor

We previously demonstrated *in vitro* differentiation of retinal photoreceptor cells from wild-type human ES [8] and iPS cells [9,10] using a stepwise differentiation method known as serum-free culture of embryoid body-like aggregates [12]. We first evaluated the differentiation efficiency of three selected iPS cell lines of the five patients (**Fig. 2A**). Retinal progenitor, photoreceptor precursor, retinal pigment epithelium (RPE) and rod photoreceptor cells were sequentially induced (**Fig. 2B–K**), consistent with our previous studies [8–10,12]. All patient-derived iPS cell lines differentiated into RPE cells that form ZO-1+ tight junctions on differentiation day 60, with timing, morphology, and efficiency similar to that of wild-type iPS cells (**Fig. 2D–E; Fig. S5**). Immature photoreceptors expressing Crx and Recoverin (day ~60) were observed as clusters in the colonies (**Fig. S6A–B**). The patient-iPS cells also differentiated into blue Opsin+ or red/green Opsin+ cone photoreceptor cells (**Fig. 2H** and data not shown). Immunostaining of Rhodopsin (a marker of mature rod photoreceptors) revealed no Rhodopsin+ cells at differentiation day 100 (data not shown). Rhodopsin+ cells appeared at differentiation day 120 with a stable efficiency of the three independent iPS cell lines from each patient (**Fig. 2K,N and Fig. S6C**). Additionally, 15.1±0.60% and 13.3±1.65% cells were positive for Recoverin (a conventional marker for both rod, cone photoreceptors and cone bipolar cells) in K21- and K11-iPS cells, respectively

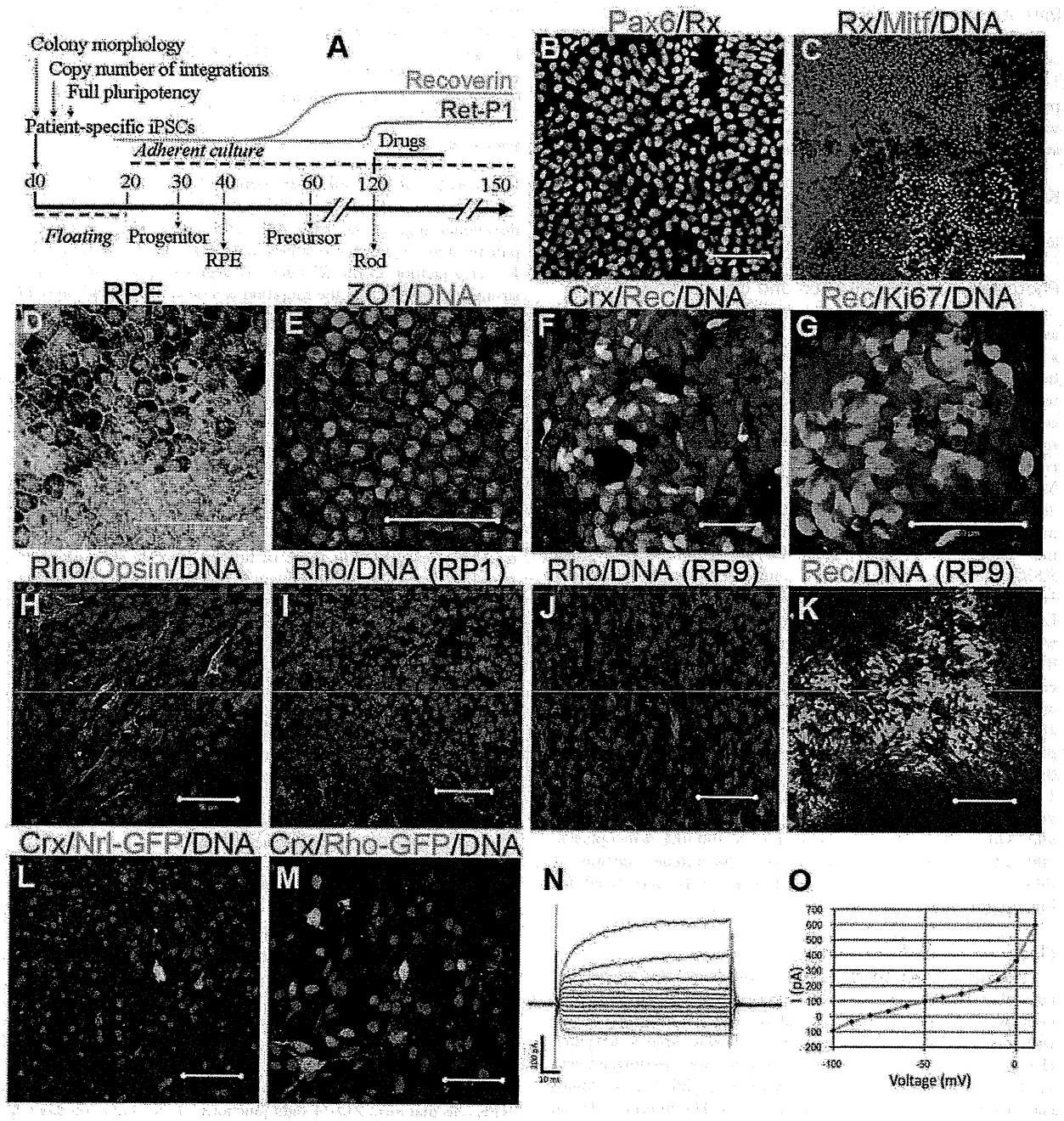

Figure 2. Induction of patient-specific retinal photoreceptor cells. Retinal cells were induced sequentially by *in vitro* differentiation. **(A)** Experimental schema. **(B)** Neural retina progenitor cells (Pax6+Rx+) and RPE progenitor cells (Mitf+) were separated in the culture dish **(C)**. Patient-specific RPE cells exhibited hexagonal morphology and pigmentation **(D)** and expressed the tight junction marker ZO-1 **(E)**. Photoreceptor cells were positive for immature photoreceptor markers Crx and Recoverin on day 60 **(F)**. Recoverin+ cells did not co-express Ki67, a proliferating cell marker **(G)**. Differentiation of rod photoreceptors (Rhodopsin+) and cone photoreceptors (Opsin+) from patient iPS cells **(H)**. Rhodopsin + rod photoreceptors induced from K21-iPS at day 120 **(I)**. K11-derived rod photoreceptors were observed at day 120 **(J)**. No Rhodopsin+ cells were detected, but Recoverin+ cells were present at day 150**(K)**. Induced rod photoreceptor cells (Crx+) labeled with lentiviral vectors encoding GFP driven by a rod photoreceptor-specific promoter Nrl **(L**: Nrl-GFP) or Rhodopsin **(M**: Rho-GFP). Arrows indicate cells co-expressing Crx and GFP. **(N)** Whole-cell recording of rod photoreceptor cell differentiated human iPS cells. Recorded cells expressed GFP under the control of the Rhodopsin promoter. **(O)** Relationship between voltage and membrane current (i) produced a non-linear curve, suggesting that voltage-dependent channels exist in iPS cell-derived rod photoreceptors Rec, Recoverin; Rho, Rhodopsin. Scale bars, 50 μm.
doi:10.1371/journal.pone.0017084.g002

(data from three selected lines), consistent with stable differentiation. Furthermore, we confirmed rod induction by labeling with lentiviral vectors driving GFP from the Rhodopsin and Nrl promoters, either of which is specifically expressed in rod photoreceptors (**Fig. 2L–M**). Whole-cell patch-clamp recording demonstrated that the rod photoreceptor cell membrane contains voltage-dependent channels, suggesting that differentiated patient-derived rod cells are electrophysiologically functional (**Fig. 2N–O**). Meanwhile, the excluded iPS cell lines (ones that showed spontaneous differentiation during maintenance, or had a high copy number of transgenes), demonstrated a significant diversity of differentiation (**Fig. S7**). Together, these data show that patient-derived iPS cells can differentiate into cells that exhibit many of the immunochemical and electrophysiological features of mature rod photoreceptor cells.

Patient-specific rod cells undergo degeneration *in vitro*

As compared with normal iPS cells, there is no significant difference in rod cell differentiation efficiency at day 120 in K21(RP1)-, P101(PRPH2)-, and P59(RHO)-iPS cell lines (**Fig. 3**). iPS cells from both K11(RP9) and K10(RP9) carried a RP9 mutation; however, rod cell number was significantly lower than in normal iPS cells (**Fig. 3**). We asked whether early death of precursor cells leads to a smaller number of mature rod photoreceptor cells. To determine whether genetic mutations induce degeneration in photoreceptors cells *in vitro*, we extended the culture period and evaluated the number of rod photoreceptors at day 150. In differentiated iPS cells from patient K21(RP1) at day 150, the number of Rhodposin+ cells was significantly decreased (**Fig. 3**). For the K11-iPS cells, no Rhodposin+ cells were found at day 150 (**Fig. 3**). Importantly, some K11-cells at day 150 were positive for Recoverin (10.3±1.99%) and Crx, markers for the rod, cone photoreceptors, and/or bipolar cells (**Fig. 2K** and data not shown), strongly suggesting that cone photoreceptor and/or bipolar cells survived, whereas the rod photoreceptors underwent degeneration *in vitro*. In addition, we detected cells positive for Islet1 (a marker for retinal amacrine, bipolar and ganglion cells), again consistent with the survival of other types of retinal cells (**Fig. S6F**). From these results, we concluded that mature rod photoreceptors differentiated from patient iPS cells selectively degenerate in an RP-specific manner *in vitro*.

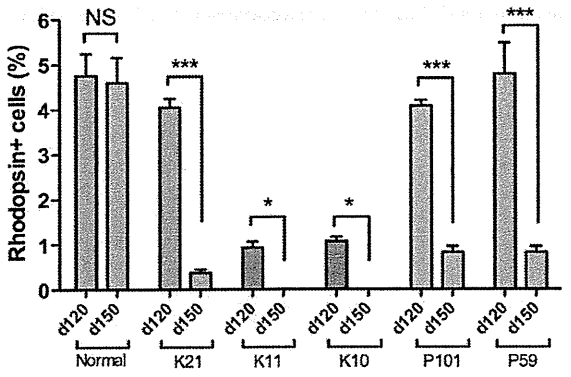

Figure 3. RP patient-derived rod photoreceptors undergo degeneration *in vitro*. iPS cells were differentiated into Rhodopsin+ rod photoreceptors in serum-free culture of embryoid body-like aggregates (SFEB culture). The percentages of Rhodopsin+ rod photoreceptors were evaluated at both day 120 and day 150, respectively. Data were from three independent iPS cell lines derived from the patients. ANOVA followed by Dunnett's test. * $p<0.05$; *** $p<0.001$. Values in the graphs are means and s.e.m.
doi:10.1371/journal.pone.0017084.g003

Cellular stresses involved in patient-derived rod cells

We next asked how the patient-derived rod photoreceptors degenerate. We evaluated apoptosis and cellular stresses in each cell line at both day 100 and day 120, respectively. Interestingly, in the RP9-iPS (K10 and K11) cells, a subset of Recoverin+ cells co-expressed cytoplasmic 8-hydroxy-2'-deoxyguanosine (8-OHdG), a major oxidative stress marker, indicating the presence of DNA oxidation in RP9 patient-derived photoreceptors by differentiation day 100 (**Fig. 4A** and **Fig. S8**). More caspase-3+ cells were presented in the Crx+ photoreceptor cluster of RP9-iPS than in those from other lines (**Fig. 4C–D**). After maturation of the rod photoreceptors from RP9-iPS cells, Rhodopsin+ cells co-expressed Acrolein, a marker of lipid oxidation (**Fig. 4E**), while no Rhodopsin+/Acrolein+ cells were observed in iPS cells derived from other patients carrying different mutations or in normal iPS cells (**Fig. 4F**). This pattern was similar to the cases of 8-OHdG and activated caspase-3. Thus, we conclude that oxidation is involved in the RP9-rod photoreceptor degeneration.

In differentiated RHO-iPS (P59) cells, we found that Rhodopsin proteins were localized in the cytoplasm (**Fig. 4G**), as determined by immunostaining with anti-Rhodopsin antibody (Ret-P1). This pattern is unlike the normal localization of Rhodopsin at the cell membrane in photoreceptors derived from normal iPS or other patient-derived iPS cells (**Fig. 4H** and data not shown). This result suggests accumulation of unfolded Rhodopsin, as reported previously in rhodopsin mutant mice cells [13]. We next examined the possible involvement of endoplasmic reticulum (ER) stress in RHO-iPS cell line degeneration. The Rhodopsin+ or Recoverin+ cells co-expressed immunoglobulin heavy-chain binding protein (BiP) or C/EBP homologous protein (CHOP), two conventional markers of endoplasmic reticulum (ER) stress, from day 120 (**Fig. 4I,K and Fig. S9**), while cells derived from control iPS or other mutant iPS cells were negative for BiP and CHOP (**Fig. 4J,L**). Taken together, these results demonstrate that ER stress is involved in rod photoreceptors carrying a RHO mutation.

Drug evaluation in patient-specific rod cells

The antioxidant vitamins α-tocopherol, ascorbic acid, and β-carotene have been tested in clinical trials as dietary therapies for RP [2] and in another major retinal degenerative disease, age-related macular degeneration [14]. Thus far, mostly due to the lack of appropriate validation models, there has been no evidence supporting the beneficial effects of these compounds on rod photoreceptors. We therefore assessed the effects of these agents on rod photoreceptors derived from patient iPS cells. In mouse retinal culture, short-term treatment with α-tocopherol, ascorbic acid and β-carotene at 100 μM, 200 μM and 1.6 μM, respectively, exerted no significant toxic effects on rod photoreceptor cells (**Fig. S10**). Since the differentiated rod photoreceptors underwent degeneration after day 120, we treated the cells for 7 days with these agents starting at day 120 (**Fig. 2A**). α-Tocopherol treatment significantly increased the number of Rhodopsin+ cells in iPS cells derived from K11- and K10-iPS with the RP9 mutation, while it had no significant effects on iPS cells with the either the RP1, PRPH2 or RHO mutation (**Fig. 5**). In contrast, neither ascorbic acid nor β-carotene treatment had any effect on iPS cells of any genotype (**Fig. S11**). We cannot currently explain the discrepancy between the effects of these antioxidants. It has been reported that under certain circumstances, anti-oxidants can act as "pro-oxidants" [15]. Taken together, our results indicate that treatment with α-tocopherol is beneficial to RP9-rod photoreceptor survival, and causes different effects on Rhodposin+ cells derived from different patients.

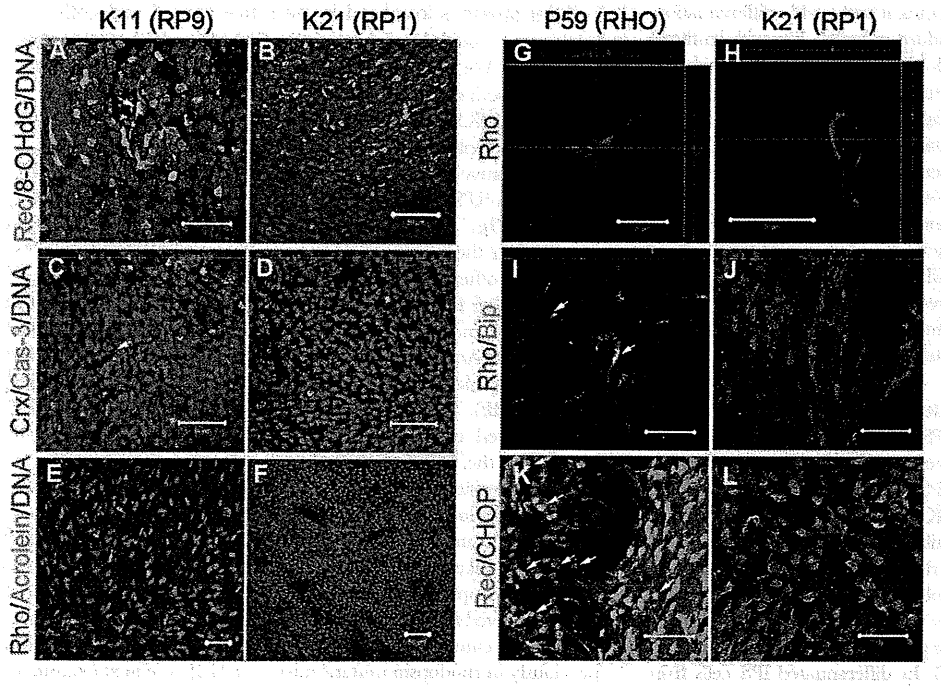

Figure 4. Cellular stress in patient-derived rod photoreceptor cells. Oxidative stress and apoptosis in differentiated rod photoreceptor cells derived from RP9-iPS (**A,C,E**) and RP1-iPS (**B,D,F**). (**A**) 8-OHdG, a marker for DNA oxidation, was found in K11- or K10-iPS–derived differentiated cells (day 100), but not in K21-iPS (**B**). Arrow indicates a cell double-positive for 8-OHdG and Recoverin. (**C**) The number of activated Caspase-3+ cells was greater in K11-iPS differentiation than in K21-iPS (**D**). From day 120, rod photoreceptor cells (Rhodopsin+) derived from RP9-iPS co-expressed the oxidative stress marker Acrolein (**E**); whereas RP1-iPS derivatives did not (**F**). (**G–L**) Abnormal cellular localization of Rhodopsin proteins and endoplasmic reticulum stress in RHO-iPS–derived rod photoreceptors. High magnification revealed cytoplasmic localization of Rhodopsin in rod photoreceptor cells carrying a RHO mutation (**G**) and a normal localization in the cell membrane in K21 cells (**H**). Rod cells derived from RHO-iPS co-expressed the ER stress markers BiP (**I**) and CHOP (**K**). K21-iPS–derived rod cells did not express BiP (**J**) or CHOP (**L**). Arrows indicate double-positive cells. Rec, Recoverin; Rho, Rhodopsin. All scale bars are 50 μm except for G and H (20 μm).
doi:10.1371/journal.pone.0017084.g004

Discussion

By using patient-derived iPS cells and *in vitro* differentiation technology, we have shown that RP9-retinitis pigmentosa is involved, at least in part, in oxidative stress pathways; this has not been reported previously in any animals or cell models. Furthermore, we have demonstrated that the antioxidant α-tocopherol exerts a beneficial effect on RP9-rod cells. Additionally, we have clearly shown that rod photoreceptors derived from patients with a RHO mutation are associated with ER stress; this is

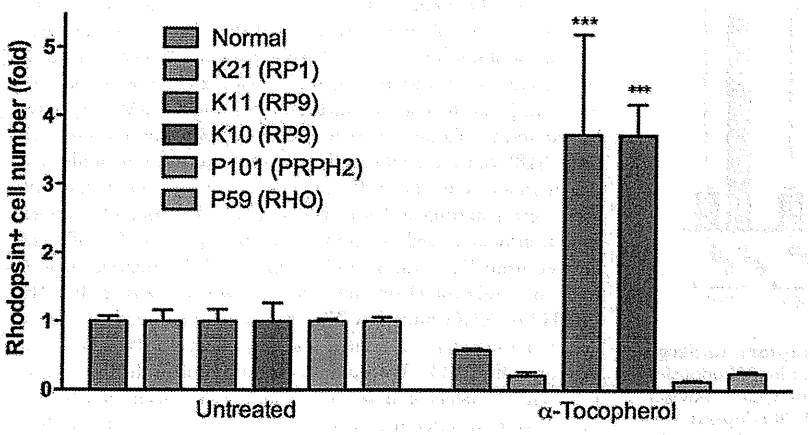

Figure 5. Disease modeling of patient-derived rod photoreceptor cells. α-Tocopherol treatment of patient-specific rod photoreceptors yielded a significant beneficial effect in RP9 mutant cells. Two-way ANOVA Bonferroni post-test showed no significance in other group (n = 3–8). Data represent 1–2 selected iPS cell lines of each patient. ***$p<0.001$. Values in the graphs are means and s.e.m.
doi:10.1371/journal.pone.0017084.g005

the first report of ER stress in a cell culture model for human rod cells. These cell models will be very useful for disease mechanism dissection and drug discovery. By screening several drugs that had already been tested in RP patients, we have revealed that rod photoreceptor cells derived from RP patients with different genetic subtypes exhibit significant differences in drug responses. Among the different types of antioxidants, α-tocopherol has either beneficial or non-beneficial effects on diseased photoreceptors, depending on the genetic mutation. This is the first report of the utilization of iPS cells related to personalized medicine, which will be helpful for routin clinical practice. Our results also provided evidence that genetic diagnosis is essential for optimizing personalized treatment for patients with retinal degenerative diseases [11]. An important future study made possible by this work is the screening of a compound library for drugs that could be used to treat RP. Patient-derived iPS cells revealed differences in pathogenesis and the efficacy of antioxidants among patients with different disease-causing mutations. Although the microenvironment affects the pathogenesis of diseases, and *in vitro* evaluation is not perfect, this study suggests that iPS cells could be used to select between multiple available treatments, allowing physicians to advise each patient individually. The weakness of our method for disease modeling is that differentiation requires a long period of time. Shortening the induction period and identifying appropriate surface markers for rod cells will improve disease modeling using patient-specific iPS cells.

In brief, we generated pluripotent stem cells from retinitis pigmentosa patients and induced them into retinal cells. Compared with normal cells, patient-derived rod cells simulated the disease phenotype and exhibited different responses to specific drugs. We found that patient-specific rod cells underwent degeneration *in vitro*, which maybe related to different cellular stresses. To our knowledge, this is the first report of disease modeling of retinal degeneration using patient-derived iPS cells.

Supporting Information

Figure S1 Pedigrees of K21 (A), P59 (B), K10 and K11 (C). Families of P59 (**B**) and K10 and K11 (**C**) show autosomal dominant mode of inheritance. (**C**) Mutation analysis was performed in four patients and two normal relatives in the RP9 family. The H137L mutation in RP9 gene was co-segregated with the disease in the family. Closed symbols indicate individuals with RP and open symbols indicate unaffected subjects. Question marks indicate symptom unknown. The bars above the symbols indicate examined subjects. Arrow, proband; slash, deceased.
(TIF)

Figure S2 Mutation in the *RP9* gene. (**A**) Alignment of RP9 sequence and pseudo-gene shows the same nucleotide in the mutated location. (**B**) Sequence chromatogram of cDNA sequence demonstrates the c.410A>T (H137L) mutation in the *RP9* gene, instead of the paralogous variant in pseudo-gene which was documented in RetNet (www.sph.uth.tmc.edu/retnet/disease.htm).
(JPG)

Figure S3 Selection by colony morphology. (**A**) iPS colony (K21S4) shows ES-like morphology. (**B**) Spontaneous differentiation in the colony during maintenance (K21S14). Scale bars, 50 μm.
(TIF)

Figure S4 Quantification of transgene copy number. Total copy number of four transgenes in the selected iPS lines. Selected iPS cells with fewest integrations and two high copy number lines used for *in vitro* differentiation.
(TIF)

Figure S5 Efficiency of RPE induction in patient-iPS cells. RPE production of the five patient-iPS cells showed no significant differences (n = 4). Data represent the percentage of RPE area at differentiation day 60. One-way ANOVA followed by Dunnett's test. Values are mean and s.e.m.
(TIF)

Figure S6 Induced retinal cells from patient iPS cells (K21S4). Crx+ photoreceptor precursor cells present in the cell cluster on differentiation day 60 (A). Crx+ cells co-expressed Recoverin, indicating differentiation into photoreceptor cells (B). Rhodopsin+ cells had a long process at day 150 (C). In the differentiated cells, we also observed cells positive of PKCα (a marker for bipolar cells) (D). Cells positive for Math5 and Brn3b (markers for ganglion progenitor or ganglion cells (day 60) (E). Cells positive for Islet-1 (a marker for amacrine, bipolar and ganglion cells) (F). Scale bars, 50 μm (A, D, E, and F); 20 μm (B and C).
(TIF)

Figure S7 Differentiation of the patient-iPS cells. iPS colony was cut into uniform sized pieces (**A**) and subjected to a floating culture (P59M8, day 20) (**B**). RPE (pigmented) and recoverin+ (green) cells were efficiently induced (P59M8, day 60) (**C**). (**D**) An excluded iPS line, P59M16, with high number transgenes showed a striking lentoid formation during the floating culture (day 20). Scale bars, 50 μm.
(TIF)

Figure S8 Oxidative stress in photoreceptor cells with the RP9 mutation (K11). (A) Recoverin, (B) 8-OHdG, (C) Recoverin/8-OHdG, (D) Recoverin/8-OHdG/DNA. Arrows indicate cells with weak Recoverin signal positive for 8-OHdG; Arrowheads represent cells with strong Recoverin signal positive for 8-OHdG; Asterisks represent Recoverin+ cells negative for 8-OHdG. Scale bar, 50 μm.
(JPG)

Figure S9 ER stress in photoreceptor cells with the RHO mutation (P59). (A) CHOP, (B) Recoverin, (C) Recoverin/CHOP, (D) Recoverin/CHOP/DNA. Arrows indicate cells with weak Recoverin signals positive for CHOP in nuclei; Arrowheads represent cells with strong Recoverin signals positive for CHOP; Asterisks represent Recoverin+ cells negative for CHOP. Scale bar, 50 μm.
(JPG)

Figure S10 Toxicity testing of the antioxidants in murine retina-derived rod photoreceptor cells. Primary culture of mouse retinal cells treated with 100 μM α-tocopherol, 200 μM ascorbic acid or 1.6 μM β-carotene for 24 hours and the rod photoreceptors were counted using flow cytometry. Value represents the ratio of treated-rod photoreceptors compared with control cells. n = 4. One-way ANOVA followed by Dunnett's test. Values are mean and s.e.m. NS, not significant.
(JPG)

Figure S11 Differentiated rod cells from normal and patient iPS cells treated with 200 μM ascorbic acid or 1.6 μM β-carotene did not show statistically significant differences. Two-way ANOVA Bonferroni post-test. Values are mean and s.e.m.
(JPG)

Table S1 Phenotypic data of the RP patients. M, male; F, female; AD, age at diagnosis; BCVA, best corrected visual acuity; HM, hand motion.
(DOC)

Table S2 Antibodies used in the present study.
(DOC)

Acknowledgments

We thank C. Ishigami and Y. Tada for assistance of mutation screening; K. Iseki, N. Sakai, Y. Wataoka, K. Sadamoto, A. Tachibana, C. Yamada for technical assistance; Y. Arata, W. Meng, C. Li, A. Suga, M. Mandai and all members in the Takahashi lab for advice.

Author Contributions

Conceived and designed the experiments: ZBJ MT. Performed the experiments: ZBJ SO FO KH JA. Analyzed the data: ZBJ SO FO. Contributed reagents/materials/analysis tools: MT YH TI. Wrote the paper: ZBJ MT.

References

1. Weleber RG, Gregory-Evans K (2006) Retimtis Pigmentosa and Allied Disorders. In: Hilton DR, Schachat AP, Ryan SJ, eds. Retina. Elsevier Mosby. pp 395–498.
2. Berson EL, Rosner B, Sandberg MA, Hayes KC, Nicholson BW, et al. (1993) A randomized trial of vitamin A and vitamin E supplementation for retinitis pigmentosa. Arch Ophthalmol 11: 761–772.
3. Takahashi K, Tanabe K, Ohnuki M, Narita M, Ichisaka T, et al. (2007) Induction of pluripotent stem cells from adult human fibroblasts by defined factors. Cell 131: 861–872.
4. Yu J, Vodyanik MA, Smuga-Otto K, Antosiewicz-Bourget J, Frane JL, et al. (2007) Induced pluripotent stem cell lines derived from human somatic cells. Science 318: 1917–1920.
5. Park IH, Arora N, Huo H, Maherali N, Ahfeldt T, et al. (2008) Disease-specific induced pluripotent stem cells. Cell 134: 877–886.
6. Raya A, Rodríguez-Pizà I, Guenechea G, Vassena R, Navarro S, et al. (2009) Disease-corrected haematopoietic progenitors from Fanconi anaemia induced pluripotent stem cells. Nature 460: 53–59.
7. Yamanaka S (2007) Strategies and new developments in the generation of patient-specific pluripotent stem cells. Cell Stem Cell 1: 39–49.
8. Osakada F, Ikeda H, Mandai M, Wataya T, Watanabe K, et al. (2008) Toward the generation of rod and cone photoreceptors from mouse, monkey and human embryonic stem cells. Nat Biotechnol 26: 215–224
9. Osakada F, Jin ZB, Hirami Y, Ikeda H, Danjyo T, et al. (2009) In vitro differentiation of retinal cells from human pluripotent stem cells by small-molecule induction. J Cell Sci 122: 3169–3179.
10. Hirami Y, Osakada F, Takahashi K, Okita K, Yamanaka S, et al. (2009) Generation of retinal cells from mouse and human induced pluripotent stem cells. Neurosci Lett 458: 126–131.
11. Jin ZB, Mandai M, Yokota T, Higuchi K, Ohmori K, et al. (2008) Identifying pathogenic genetic background of simplex or multiplex retinitis pigmentosa patients: a large scale mutation screening study. J Med Genet 45: 465–472.
12. Ikeda H, Osakada F, Watanabe K, Mizuseki K, Haraguchi T, et al. (2005) Generation of Rx+/Pax6+ neural retinal precursors from embryonic stem cells. Proc Natl Acad Sci U S A 102: 11331–11336.
13. Sung CH, Davenport CM, Nathans J (1993) Rhodopsin mutations responsible for autosomal dominant retinitis pigmentosa. Clustering of functional classes along the polypeptide chain. J Biol Chem 268: 26645–26649.
14. van Leeuwen R, Boekhoorn S, Vingerling JR, Witteman JC, Klaver CC, et al. (2005) Dietary intake of antioxidants and risk of age-related macular degeneration. JAMA 294: 3101–3107.
15. van Helden YG, Keijer J, Heil SG, Picó C, Palou A, et al. (2009) Beta-carotene affects oxidative stress-related DNA damage in lung epithelial cells and in ferret lung. Carcinogenesis 30: 2070–2076.

One case of peripheral ulcerative keratitis (Leroux et al. 2004) and one case of paralimbal keratitis caused by candida glabrata (Djalilian et al. 2001) have been reported in patients with CGD. However, no case with so centrally positioned infiltrate and such deterioration of BCVA has been reported. The negative culture can be interpreted as noninfectious infiltrate in the left cornea, but the profound clinical and subjective improvement after the prescription of levofloxacin drops implies the opposite. The fact that antibiotic drops were prescribed 2 days earlier can perhaps explain the negative culture, as this can interfere with microbiology testing. The other possibility but less likely would be a sterile inflammatory keratitis (maybe related to granuloma formations already known in other organs), which has not been described earlier in such patients. Regarding other possible systemic causes of granulomas, the patient has regular contact with infection clinic, and no other infections have been diagnosed.

References

Djalilian AR, Smith JA, Walsh TJ, Malech HL & Robinson MR (2001): Keratitis caused by Candida glabrata in a patient with chronic granulomatous disease. Am J Ophthalmol **132**: 782–783.

Goldblatt D, Butcher J, Thrasher AJ & Russell-Eggitt I (1999): Chorioretinal lesions in patients and carriers of chronic granulomatous disease. J Pediatr **134**: 780–783.

Johnston RB Jr (2001): Clinical aspects of chronic granulomatous disease. Curr Opin Hematol **8**: 17–22.Review.

Kim SJ, Kim JG & Yu YS (2003): Chorioretinal lesions in patients with chronic granulomatous disease. Retina **23**: 360–365.

Leroux K, Mallon E & Ayliffe WH (2004): Chronic granulomatous disease and peripheral ulcerative keratitis: a rare case of recurrent external ocular disease. Bull Soc Belge Ophtalmol **293**: 47–53.

Correspodence:
Dr Marios Panagiotopoulos
Department of Ophthalmology
Örebro University Hospital
70185 Örebro
Sweden
Tel: + 46 19 6021000
Fax: + 46 19 6021052
Email: marios.panagiotopoulos@orebroll.se

Stargardt Disease with Preserved Central Vision: identification of a putative novel mutation in ATP-binding cassette transporter gene

Kaoru Fujinami,[1] Masakazu Akahori,[2] Masaki Fukui,[1] Kazushige Tsunoda,[1] Takeshi Iwata,[2] and Yozo Miyake[1,3]

[1]Laboratory of Visual Physiology, National Institute of Sensory Organs, Meguro-ku, Tokyo, Japan
[2]Division of Molecular & Cellular Biology, National Institute of Sensory Organs, National Hospital Organization, Tokyo Medical Center, Meguro-ku, Tokyo, Japan
[3]Aichi Shukutoku University, Aichi, Japan, Nagakute-cho, Aichi-gun, Aichi, Japan

doi: 10.1111/j.1755-3768.2009.01848.x

Editor,

Stargardt disease (STGD) has a juvenile to young–adult onset, a rapid decrease of central vision and a progressive bilateral atrophy of the sensory retina and retinal pigment epithelium (RPE) in the macula. Yellow-orange flecks are often detected around the macula, the midretina and or both (Rotenstreich et al. 2003). Mutations in the gene encoding the ATP-binding cassette transporter gene (ABCA4) are responsible for autosomal recessive STGD (Allikmets 1997; Webster et al. 2001). We examined a patient who had the characteristic signs of STGD but had good visual acuity.

A 66-year-old man complained of photophobia and a paracentral scotoma which was present since his teens and had not worsened. None of his family members had similar symptoms. His visual acuity was 20/15 OU, and ophthalmoscopy identified a dark brown, well-demarcated area at the fovea surrounded by RPE atrophy and flecks (Fig. 1A). Fluorescein angiography showed window defects at the flecks and a dark choroid (Fig. 1B). The optical coherence tomographic (OCT) images showed a well-preserved sensory retina and normal thickness RPE at the fovea (Fig. 1C, D). The foveal area was surrounded by atrophic sensory retina and RPE. Static perimetry showed ring-shaped paracentral relative scotoma which surrounded the normal area seeing area of 5° (Fig. 1E). Focal macular electroretinograms (FMERGs) also demonstrated a well-preserved retinal function at the fovea (Fig. 1F). Compared to age-matched controls, the FMERGs had normal responses elicited by a 5-degree stimulus spot and severely reduced responses elicited by 10-degree and 15-degree spots (Fig. 1F, G). Genetic analysis with direct DNA sequencing of amplified products revealed four reported polymorphisms (Allikmets 1997; Briggs et al. 2001; Webster et al. 2001; Fukui et al. 2002) and one novel mutation, Met280Thr, in exon 7 of the ABCA4 gene (Table 1).

Our patient had clinical findings that were pathognomonic of typical STGD, except that the clinical course was stationary and he had 20/15 vision because of well-preserved foveal function. The preserved foveal area was small and well demarcated. Visual acuity, fundus appearance, OCT images, static perimetry and FMERGs supported the well-preserved foveal function. We report our case because the patient had a unique phenotype with a novel putative mutation in the *ABCA4* gene, not yet shown to segregate with the disease.

The well-demarcated dark brown foveal RPE appeared to be hyperpigmented although the thickness measured by OCT was 29 μm which was within normal limits. The findings in our case could indicate that the non-atrophic foveal RPE had an effect in preserving the foveal morphology and function.

The inheritance of STGD is autosomal recessive; however, our patient had four polymorphisms and one heterozygous gene mutation c.839T>C in exon 7 in the *ABCA4* gene. A second mutation was not found, but it may well exist outside of the coding sequence of the *ABCA4* gene. The new mutation in our patient was located outside the known functional domains of ATP-binding or transmembrane site (Lewis et al. 1999), which may explain the mild effect of the missense mutation. We should

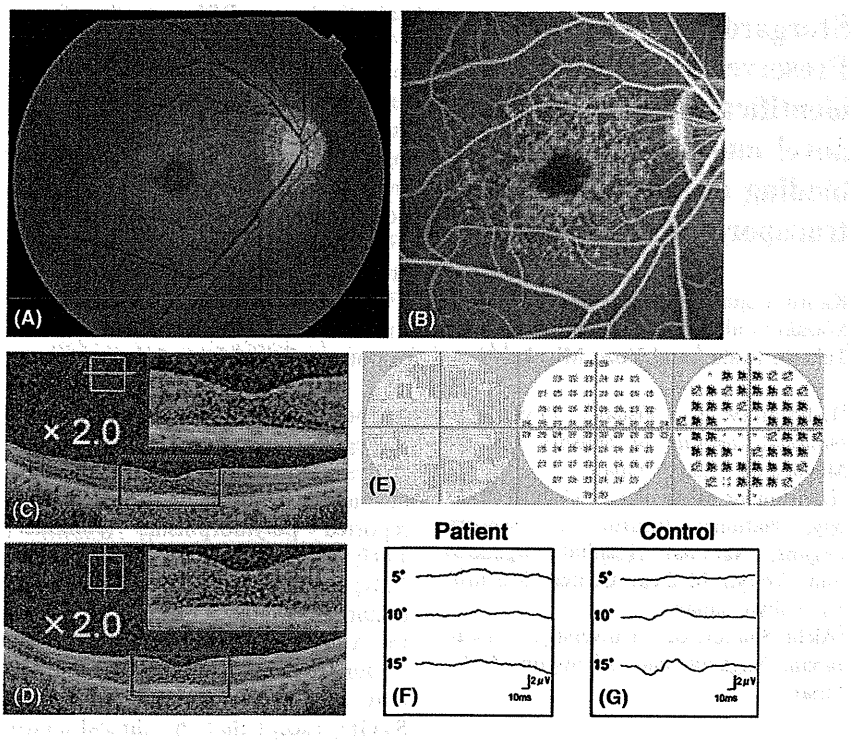

Fig. 1. Fundus photograph (A), fluorescein angiogram (FA) (B), optical coherence tomography (OCT) (C, D), Humphrey static perimetry (E), and focal macular electroretinograms (FMERGs) (F) of an eye of a patient with Stargardt disease. (A) Fundus photograph showing dark brown, well demarcated area in the fovea surrounded by orange-yellow flecks in the macula. (B) FA showing blockage in the foveal area, ring-shaped mottled hyperfluorescence in the macula, and dark choroid. (C, D) OCT images (C; horizontal, D; vertical) showing well-preserved sensory retina and retinal pigment epithelium (RPE) layer in the fovea. In the juxtafoveal region, an atrophy of both sensory retina and RPE can be seen. The enlarged images within the red lines are attached. (E) Humphrey static perimetry showing ring-shaped paracentral relative scotoma (10-2 strategy). (F, G) FMERGs showing normal responses elicited by a 5-degree stimulus spot and severely reduced responses elicited by 10-degree and 15-degree spots, when compared with the age-matched control.

Table 1. ABCA4 GENE MUTATION AND Polymorphisms.

Exon	Nucleotide Change	Effect Changes	Het/Hom	References
Mutation				
7	c.839T > C	p.Met280Thr	Het	Present study
Polymorphisms				
10	c.1269C > T	p.His424His	Hom	Webster AR et al.
45	c.6249C > T	p.Ile2083Ile	Het	Allikmets R et al.
46	c.6285T > C	p.Asp2095Asp	Het	Briggs CE et al.
49	c.6764G > T	p.Ser2255Ile	Het	Allikmets R et al.

The translational start codon ATG/methionine is numbered as +1. One novel disease-associated mutation [c.839T > C (p.Met280Thr)] was found. References of previously reported polymorphisms are indicated.
Het, heterozygote; Hom, homozygote.

also consider a modifier gene effect in our patient.

Although the relationship between the new mutation of the *ABCA4* gene and the well-preserved foveal structure is unresolved, the unique phenotype and genotype of our patient may give additional information on the mechanism of photoreceptor degeneration in eyes with STGD.

References

Allikmets R (1997): A photoreceptor cell-specific ATP-binding transporter gene (ABCR) is mutated in recessive Stargardt macular dystrophy. Nat Genet **17**: 122.

Briggs CE, Rucinski D, Rosenfeld PJ, Hirose T, Berson EL & Dryja TP (2001): Mutations in ABCR (ABCA4) in patients with Stargardt macular degeneration or cone-rod degeneration. Invest Ophthalmol Vis Sci **42**: 2229–2236.

Fukui T, Yamamoto S, Nakano K et al. (2002): ABCA4 gene mutations in Japanese patients with Stargardt disease and retinitis pigmentosa. Invest Ophthalmol Vis Sci **43**: 2819–2824.

Lewis RA, Shroyer NF, Singh N et al. (1999): Genotype/Phenotype analysis of a photoreceptor-specific ATP-binding cassette transporter gene, ABCR, in Stargardt disease. Am J Hum Genet **64**: 422–434.

Rotenstreich Y, Fishman GA & Anderson RJ (2003): Visual acuity loss and clinical observations in a large series of patients with Stargardt disease. Ophthalmology **110**: 1151–1158.

Webster AR, Heon E, Lotery AJ et al. (2001): An analysis of allelic variation in the ABCA4 gene. Invest Ophthalmol Vis Sci **42**: 1179–1189.

Correspondence:
Kazushige Tsunoda, MD
Laboratory of Visual Physiology
National Institute of Sensory Organs
2-5-1 Higashigaoka
Meguro-ku
Tokyo 152-8902
Japan
Tel: + 81 3 3411 0111 ext. 6615
Fax: + 81 3 3412 9811
Email: tsunodakazushige@kankakuki.go.jp

Molecular Vision 2011; 17:3309-3313 <http://www.molvis.org/molvis/v17/a356>
Received 31 July 2011 | Accepted 14 December 2011 | Published 17 December 2011

Analysis of *LOXL1* gene variants in Japanese patients with branch retinal vein occlusion

Katsunori Hara,[1] Masakazu Akahori,[2] Masaki Tanito,[1] Sachiko Kaidzu,[1] Akihiro Ohira,[1] Takeshi Iwata[2]

(The first two authors contributed equally to this work)

[1]Department of Ophthalmology, Shimane University Faculty of Medicine, Izumo, Shimane, Japan; [2]National Institute of Sensory Organs, National Hospital Organization Tokyo Medical Center, Tokyo, Japan

Purpose: Previous studies have described a possible association between exfoliation syndrome (EX) and various ocular and systemic vascular disorders; however, the association between EX and branch retinal vein occlusion (BRVO) remains unclear. Because slit-lamp examination may overlook latent deposits of exfoliation materials, an ocular biopsy is usually needed for a precise diagnosis. We evaluated a possible association between EX and BRVO using lysyl oxidase-like 1 (*LOXL1*) gene variants as alternative markers for EX.

Methods: Allelic and genotypic frequencies of three *LOXL1* variants (rs1048661, rs3825942, and rs2165241) were determined for 78 consecutive Japanese patients with BRVO (11 patients with exfoliation syndrome [EX+], 67 patients without exfoliation syndrome [EX-]), and 158 patients with cataract without EX (CT) as controls.

Results: The rs1048661 variant differed between the BRVO and CT groups in allelic and genotypic frequencies (p=0.0137 and p=0.0203, respectively). Subgroup analysis, compared to the CT group, showed that BRVO EX+ had significantly different allelic and genotypic frequencies of rs1048661 (p=0.00011 and p=0.000189, respectively), while BRVO EX- did not (p=0.175 and p=0.288, respectively). The frequencies of rs3825942 and rs2165241 did not differ between the BRVO and CT groups.

Conclusions: No association was found between BRVO and EX if *LOXL1* variants were used as disease markers for clinically undetectable EX. The results suggested that *LOXL1* variants, well established markers for EX, are not likely genetic markers for BRVO in Japanese subjects.

Retinal vein occlusions (RVOs), including central retinal vein occlusion (CRVO), an occlusion at the central trunk of the retinal vein, and branch retinal vein occlusion (BRVO), an occlusion at an arteriovenous crossing where the retinal artery and vein are bound by a common adventitial sheath, are important causes of ocular morbidity [1,2]. Although CRVO and BRVO have several risk factors in common, including systemic hypertension, smoking, hyperlipidemia, and elevated plasma homocysteine [1,2], they do not fully explain the involvement of the central trunk or branch of the retinal vein circulation.

Exfoliation syndrome (EX), the most common identifiable cause of open-angle glaucoma worldwide, is an age-related, generalized disorder of the extracellular matrix characterized by the production and progressive accumulation of fibrillar extracellular material in many ocular tissues [3]. A recent genome-wide association study reported that one intronic single nucleotide polymorphism (SNP; rs2165241) and two exonic SNPs (rs1048661 [R141L], rs3825942 [G153D]) in the first exon of the lysyl oxidase-like 1 *(LOXL1)* gene on chromosome 15q24.1 are highly associated with EX in Icelandic and Swedish populations, and that none of these SNPs was associated with primary open-angle glaucoma in the two populations [4]. Several studies have confirmed the association of these SNPs with EX in other populations [5], including a Japanese population [6-11].

In addition to ocular tissues, production and progressive accumulation of exfoliation materials occur in skin and various visceral organs [3,12]. The association of EX with various systemic vascular and neurodegenerative disorders has been described in ischemic heart disease [13,14], carotid stiffness [15], cerebrovascular disease [16], Alzheimer disease [17], and hearing loss [18]. Regarding RVO, several studies have described a possible association between CRVO and EX diagnosed based on chart review [19], slit-lamp examination [20], histopathologic studies in enucleated eyes [21,22], and a combination of slit-lamp examination and conjunctival biopsy [23], while only a few studies have evaluated the association between BRVO and EX [19,20]. Recently, the role of the *LOXL1* polymorphism has been tested in several ocular [24] and systemic [25,26] pathologies to explore the association between EX and these pathologies, suggesting the usefulness of analyzing *LOXL1* variants as a disease marker for EX.

Correspondence to: Masaki Tanito, Department of Ophthalmology, Shimane University Faculty of Medicine, Enya 89-1, Izumo, Shimane, 693-8501, Japan; Phone: +81-853-20-2284; FAX: +81-853-20-2278; email: tanito-oph@umin.ac.jp

Table 1. Summary of study populations.

	BRVO				
	Total	EX-	EX+	CT	p-value
No. of subjets	78	67	11	158	
Men/Women					
No.	32/46	29/38	3/8	45/113	0.0568*
%	41/59	33/67	27/73	28/72	
Age (years)					
Mean±SD	73.2±9.6	72±9.4	80.5±6.8	76.9±4.9	5.81×10^{-5}†
Range	47–88	47–87	69–88	70–90	

*Fisher's exact probability test between BRVO (total) and CT groups. †Unpaired *t*-test between BRVO (total) and CT groups.

In the current study, we tested the association between *LOXL1* variants and BRVO in a Japanese population to explore a possible association between EX and BRVO.

METHODS

Subjects: Unrelated Japanese subjects with BRVO (n=78) were consecutively recruited at the Shimane University Hospital and Iinan Hospital in Shimane, Japan. The BRVO group was divided into two subgroups based on the presence (EX+, n=11) or absence (EX-, n=67) of clinically detectable ocular deposits of exfoliation material. The data set from patients with cataract without deposits of exfoliation material (CT, n=158) reported in our previous study [11] served as a control. The demographic data including age and gender for each group are summarized in Table 1.

Methods: The current study adhered to the tenets of the Declaration of Helsinki. The institutional review boards of both hospitals reviewed and approved the research. All subjects provided written informed consent. All subjects underwent a dilated pupil examination of the anterior segments, ocular media, and fundus using a slit-lamp (RO5000, Buchmann Deutschland, Düsseldorf, Germany) and a funduscope (BS-III, Neitz Instruments, Tokyo, Japan). BRVO was diagnosed if the fundus examination revealed venous dilation and tortuosity with flame-shaped and dot-blot hemorrhages in a wedge-shaped region. Patients with CRVO and hemi-CRVO were excluded. Deposits of exfoliation material were identified if the slit-lamp examination revealed a typical pattern of exfoliation material on the anterior lens surface and/or pupillary margin.

DNA genotyping: Genomic DNA was extracted from the peripheral white blood cells of each subject. A polymerase chain reaction was performed using primers designed to amplify the genomic region containing both rs1048661 and rs3825942 (forward primer: 5′-AGG TGT ACA GCT TGC TCA ACT C-3′ and reverse primer: 5′-TAG TAC ACG AAA CCC TGG TCG T-3′) or only rs2165241 (forward primer: 5′-AGA ATG CAA GAC CTC AGC ATG AG-3′ and reverse primer: 5′-TAG TGG CCA GAG GTC TGC TAA G-3′). The sequence was determined based on the dideoxy terminator method using an ABI PRISM 3130xl Genetic Analyzer (Applied Biosystems, Foster City, CA) according to the manufacturer's protocol. We used SeqScape Software version 2.5 (Applied Biosystems) to analyze the sequence alignment.

Statistical analysis: Statistical analysis was performed using R version 2.6.2. Fisher's exact test was used to compare the allele or genotype frequencies of each group with the controls.

RESULTS

The allelic and genotypic counts and frequencies of SNPs rs1048661, rs3825942, and rs2165241 within *LOXL1* are shown in Table 2. Compared to the CT group, the T allele and TT genotype frequencies of rs1048661 were higher in patients with BRVO (p=0.0137 and p=0.0203, respectively). In subgroup analysis, compared to the CT group, the group with BRVO with exfoliation material deposits (EX+) had significantly different allelic and genotypic frequencies (p=0.00011 and p=0.000189, respectively), while the group with BRVO without exfoliation material deposits (EX-) had no difference in allelic and genotypic frequencies (p=0.175 and p=0.288, respectively). Compared to the CT group, the frequencies of the G allele of rs3825942 and the C allele of rs2165241 were higher in the BRVO EX+ groups with borderline significance (p=0.0933 and p=0.0908, respectively), but the allelic and genotypic frequencies did not differ between any pairs of BRVO total or BRVO EX- and the CT group.

DISCUSSION

To the best of our knowledge, this is the first study to identify a possible association between *LOXL1* variants and BRVO. The prevalence of clinical EX increases with age, especially after age 60 [3]. Accordingly, detection of exfoliation material deposits by slit-lamp examination may overlook latent EX. Indeed, previous studies have suggested that the prevalence of exfoliation material deposits found on histopathologic assessment of ocular specimens was roughly double compared with the slit-lamp examination [27,28]. A conjunctival biopsy can detect preclinical EX that is not evident on slit-lamp examination [23]; however, because the

Table 2. Allelic and genotypic counts and frequencies of SNPs rs1048661, rs3825942, and rs2165241.

	BRVO								p-value*		
	Total		EX-		EX+		CT				
	Count	Frequency	Count	Frequency	Count	Frequency	Count	Frequency	Total versus CT	BRVO EX- versus CT	EX+ versus CT
rs1048661											
Allele											
T	86	0.566	67	0.515	19	0.864	140	0.443	0.0137	0.175	1.10×10^{-4}
G	66	0.434	63	0.485	3	0.136	176	0.557			
Genotype											
TT	24	0.316	16	0 246	8	0.727	25	0.158	0.0203	0.288	1.89×10^{-4}
TG	38	0.500	35	0.538	3	0.273	90	0.570			
GG	14	0.184	14	0.215	0	0	43	0.272			
rs3825942											
Allele											
G	131	0.862	110	0.846	21	0.955	255	0.807	0.155	0.348	0.0933
A	21	0.138	20	0.154	1	0.045	61	0.193			
Genotype											
GG	57	0.750	47	0.723	10	0.909	101	0.639	0.212	0.424	0.209
AG	17	0.224	16	0.246	1	0.091	53	0.335			
AA	2	0.026	2	0.031	0	0	4	0.025			
rs2165241											
Allele											
C	135	0.877	113	0.856	22	1.000	277	0.877	1	0.541	0.0908
T	19	0.123	19	0.144	0	0	39	0.123			
Genotype											
CC	61	0.792	50	0.758	11	1.000	123	0.778	0.765	0.685	0.335
CT	13	0.169	13	0.197	0	0	31	0.196			
TT	3	0.039	3	0.045	0	0	4	0.025			

*Fisher's exact probability test.

biopsy is invasive, it cannot be used for all patients. The role of the *LOXL1* polymorphism has been tested in several pathologies including wet and dry age-related macular degeneration and polypoidal choroidal vasculopathy in a Japanese population [24], Alzheimer disease in a Swedish population [25], and cardiovascular disease in a Hungarian population [26]. Fuse et al. found a significant association between the rs1048661 polymorphism and wet age-related macular degeneration in a Japanese population [24]. These studies encouraged us to use the *LOXL1* polymorphism as an alternative marker of clinically undetectable EX other than invasive biopsy/histopathology.

Among the three SNPs reported [4], rs1048661 has been consistently suggested as the most significant indicator of EX/glaucoma in Icelandic, Swedish, and Japanese populations [6-11]. Accordingly, our results of a significant difference in allelic and genotypic frequencies of rs1048661 between all subjects with BRVO and CT or BRVO EX+ and CT groups confirmed previous observations of the strong role of this SNP in EX. The results also suggested that using this SNP, we can detect a case–control association for EX even with such a small number of subjects (n=11) in a case group. In the same context, the other two SNPs, which showed only a borderline difference between BRVO EX+ and CT groups, may not have enough discriminatory power with this small number of subjects.

Since both the BRVO EX- and CT groups, which were classified based on slit-lamp examination as not having EX, were identical except for the presence or absence of BRVO, comparison between these two groups should provide the most reliable information about the possible role of the *LOXL1* variants in BRVO. As a result, the significant difference observed in rs1048661 between the case and control groups was canceled in the analyses between the BRVO EX- and CT groups, suggesting that the percentage of the population at risk of EX is not significantly higher in the BRVO group. A retrospective chart review reported exfoliation material deposits in 6.0% of eyes with BRVO and 6.9% of eyes with CRVO [19], suggesting a lesser extent of BRVO than CRVO in these subjects, since the BRVO/CRVO ratio was 3.2 in the general population [29]. By clinical observation of consecutive cases, the prevalence rates of EX were 8.2% in eyes with BRVO and 20.8% in eyes with CRVO compared with 5.2% in control eyes; thus the authors concluded that EX is likely a risk factor for CRVO [20]. A retrospective chart review showed that RVO occurs more frequently in eyes more affected by EX, and that the most frequent type of RVO that occurred in EX was CRVO (50%) followed by about half that prevalence of BRVO (28%) [23]. In this study, the prevalence rate of EX was 14% in eyes with BRVO from consecutive cases, which may be higher than the rate of EX in BRVO cases and normal control subjects in previous reports [19,20]. Differences in the race or age of subjects may explain the discrepancy, but this needs to be clarified. Taken together with previous studies, our results suggest that there is no direct role of *LOXL1* variants or EX in the development of BRVO in our Japanese subjects.

In summary, we tested the possible association of *LOXL1* variants with BRVO. We did not find an association between BRVO and EX if the *LOXL1* variants were used as disease markers for clinically undetectable EX.

REFERENCES

1. The Eye Disease Case-control Study Group. Risk factors for branch retinal vein occlusion. Am J Ophthalmol 1993; 116:286-96. [PMID: 8357052]
2. Cahill MT, Stinnett SS, Fekrat S. Meta-analysis of plasma homocysteine, serum folate, serum vitamin B(12), and thermolabile MTHFR genotype as risk factors for retinal vascular occlusive disease. Am J Ophthalmol 2003; 136:1136-50. [PMID: 14644226]
3. Ritch R, Schlotzer-Schrehardt U. Exfoliation syndrome. Surv Ophthalmol 2001; 45:265-315. [PMID: 11166342]
4. Thorleifsson G, Magnusson KP, Sulem P, Walters GB, Gudbjartsson DF, Stefansson H, Jonsson T, Jonasdottir A, Stefansdottir G, Masson G, Hardarson GA, Petursson H, Arnarsson A, Motallebipour M, Wallerman O, Wadelius C, Gulcher JR, Thorsteinsdottir U, Kong A, Jonasson F, Stefansson K. Common sequence variants in the LOXL1 gene confer susceptibility to exfoliation glaucoma. Science 2007; 317:1397-400. [PMID: 17690259]
5. Jonasson F. From epidemiology to lysyl oxidase like one (LOXL1) polymorphisms discovery: phenotyping and genotyping exfoliation syndrome and exfoliation glaucoma in Iceland. Acta Ophthalmol (Copenh) 2009; 87:478-87. [PMID: 19664108]
6. Hayashi H, Gotoh N, Ueda Y, Nakanishi H, Yoshimura N. Lysyl oxidase-like 1 polymorphisms and exfoliation syndrome in the Japanese population. Am J Ophthalmol 2008; 145:582-5. [PMID: 18201684]
7. Ozaki M, Lee KY, Vithana EN, Yong VH, Thalamuthu A, Mizoguchi T, Venkatraman A, Aung T. Association of LOXL1 gene polymorphisms with pseudoexfoliation in the Japanese. Invest Ophthalmol Vis Sci 2008; 49:3976-80. [PMID: 18450598]
8. Mori K, Imai K, Matsuda A, Ikeda Y, Naruse S, Hitora-Takeshita H, Nakano M, Taniguchi T, Omi N, Tashiro K, Kinoshita S. LOXL1 genetic polymorphisms are associated with exfoliation glaucoma in the Japanese population. Mol Vis 2008; 14:1037-40. [PMID: 18552979]
9. Fuse N, Miyazawa A, Nakazawa T, Mengkegale M, Otomo T, Nishida K. Evaluation of LOXL1 polymorphisms in eyes with exfoliation glaucoma in Japanese. Mol Vis 2008; 14:1338-43. [PMID: 18648524]
10. Mabuchi F, Sakurada Y, Kashiwagi K, Yamagata Z, Iijima H, Tsukahara S. Lysyl oxidase-like 1 gene polymorphisms in Japanese patients with primary open angle glaucoma and exfoliation syndrome. Mol Vis 2008; 14:1303-8. [PMID: 18636115]
11. Tanito M, Minami M, Akahori M, Kaidzu S, Takai Y, Ohira A, Iwata T. LOXL1 variants in elderly Japanese patients with exfoliation syndrome/glaucoma, primary open-angle

glaucoma, normal tension glaucoma, and cataract. Mol Vis 2008; 14:1898-905. [PMID: 18958304]

12. Streeten BW, Li ZY, Wallace RN, Eagle RC Jr, Keshgegian AA. Pseudoexfoliative fibrillopathy in visceral organs of a patient with pseudoexfoliation syndrome. Arch Ophthalmol 1992; 110:1757-62. [PMID: 1463419]
13. Bojić L, Ermacora R, Polic S, Ivanisevic M, Mandic Z, Rogosic V, Lesin M. Pseudoexfoliation syndrome and asymptomatic myocardial dysfunction. Graefes Arch Clin Exp Ophthalmol 2005; 243:446-9. [PMID: 15599584]
14. Andrikopoulos GK, Mela EK, Georgakopoulos CD, Papadopoulos GE, Damelou AN, Alexopoulos DK, Gartaganis SP. Pseudoexfoliation syndrome prevalence in Greek patients with cataract and its association to glaucoma and coronary artery disease. Eye (Lond) 2009; 23:442-7. [PMID: 17932505]
15. Irkec M. Exfoliation and carotid stiffness. Br J Ophthalmol 2006; 90:529-30. [PMID: 16556616]
16. Linnér E, Popovic V, Gottfries CG, Jonsson M, Sjogren M, Wallin A. The exfoliation syndrome in cognitive impairment of cerebrovascular or Alzheimer's type. Acta Ophthalmol Scand 2001; 79:283-5. [PMID: 11401639]
17. Janciauskiene S, Krakau T. Alzheimer's peptide: a possible link between glaucoma, exfoliation syndrome and Alzheimer's disease. Acta Ophthalmol Scand 2001; 79:328-9. [PMID: 11401652]
18. Yazdani S, Tousi A, Pakravan M, Faghihi AR. Sensorineural hearing loss in pseudoexfoliation syndrome. Ophthalmology 2008; 115:425-9. [PMID: 18187196]
19. Cursiefen C, Händel A, Schönherr U, Naumann GO. Pseudoexfoliation syndrome in patients with retinal vein branch and central vein thrombosis. Klin Monatsbl Augenheilkd 1997; 211:17-21. [PMID: 9340400]
20. Saatci OA, Ferliel ST, Ferliel M, Kaynak S, Ergin MH. Pseudoexfoliation and glaucoma in eyes with retinal vein occlusion. Int Ophthalmol 1999; 23:75-8. [PMID: 11196123]
21. Karjalainen K, Tarkkanen A, Merenmies L. Exfoliation syndrome in enucleated haemorrhagic and absolute glaucoma. Acta Ophthalmol (Copenh) 1987; 65:320-2. [PMID: 3618156]
22. Cursiefen C, Hammer T, Kuchle M, Naumann GO, Schlotzer-Schrehardt U. Pseudoexfoliation syndrome in eyes with ischemic central retinal vein occlusion. A histopathologic and electron microscopic study. Acta Ophthalmol Scand 2001; 79:476-8. [PMID: 11594982]
23. Ritch R, Prata TS, de Moraes CG, Vessani RM, Costa VP, Konstas AG, Liebmann JM, Schlotzer-Schrehardt U. Association of exfoliation syndrome and central retinal vein occlusion: an ultrastructural analysis. Acta Ophthalmol (Copenh) 2010; 88:91-5. [PMID: 19725816]
24. Fuse N, Mengkegale M, Miyazawa A, Abe T, Nakazawa T, Wakusawa R, Nishida K. Polymorphisms in ARMS2 (LOC387715) and LOXL1 genes in the Japanese with age-related macular degeneration. Am J Ophthalmol 2011; 151:550-6. [PMID: 21236409]
25. Abramsson A, Landgren S, Zetterberg M, Seibt Palmer M, Minthon L, Gustafson DR, Skoog I, Blennow K, Zetterberg H. No association of LOXL1 gene polymorphisms with Alzheimer's disease. Neuromolecular Med 2011; 13:160-6. [PMID: 21559813]
26. Holló G, Gal A, Kothy P, Molnar JM. LOXL1 gene sequence variants and vascular disease in exfoliation syndrome and exfoliative glaucoma. J Glaucoma 2011; 20:143-7. [PMID: 20436359]
27. Prince AM, Streeten BW, Ritch R, Dark AJ, Sperling M Preclinical diagnosis of pseudoexfoliation syndrome. Arch Ophthalmol 1987; 105:1076-82. [PMID: 3632416]
28. Konstas AG, Jay JL, Marshall GE, Lee WR. Prevalence, diagnostic features, and response to trabeculectomy in exfoliation glaucoma. Ophthalmology 1993; 100:619-27. [PMID. 8493003]
29. David R, Zangwill L, Badarna M, Yassur Y. Epidemiology of retinal vein occlusion and its association with glaucoma and increased intraocular pressure. Ophthalmologica 1988; 197:69-74. [PMID: 3186211]

Articles are provided courtesy of Emory University and the Zhongshan Ophthalmic Center, Sun Yat-sen University, P.R. China. The print version of this article was created on 13 December 2011. This reflects all typographical corrections and errata to the article through that date. Details of any changes may be found in the online version of the article.

CLINICAL CHARACTERISTICS OF OCCULT MACULAR DYSTROPHY IN FAMILY WITH MUTATION OF *RP1L1* GENE

KAZUSHIGE TSUNODA, MD, PHD,* TOMOAKI USUI, MD, PHD,†‡ TETSUHISA HATASE, MD, PHD,† SATOSHI YAMAI, MD,§ KAORU FUJINAMI, MD,* GEN HANAZONO, MD, PHD,* KEI SHINODA, MD, PHD,*¶ HISAO OHDE, MD, PHD,** MASAKAZU AKAHORI, PHD,* TAKESHI IWATA, PHD,* YOZO MIYAKE, MD, PHD*††

Purpose: To report the clinical characteristics of occult macular dystrophy (OMD) in members of one family with a mutation of the *RP1L1* gene.

Methods: Fourteen members with a p.Arg45Trp mutation in the *RP1L1* gene were examined. The visual acuity, visual fields, fundus photographs, fluorescein angiograms, full-field electroretinograms, multifocal electroretinograms, and optical coherence tomographic images were examined. The clinical symptoms and signs and course of the disease were documented.

Results: All the members with the *RP1L1* mutation except one woman had ocular symptoms and signs of OMD. The fundus was normal in all the patients during the entire follow-up period except in one patient with diabetic retinopathy. Optical coherence tomography detected the early morphologic abnormalities both in the photoreceptor inner/outer segment line and cone outer segment tip line. However, the multifocal electroretinograms were more reliable in detecting minimal macular dysfunction at an early stage of OMD.

Conclusion: The abnormalities in the multifocal electroretinograms and optical coherence tomography observed in the OMD patients of different durations strongly support the contribution of *RP1L1* mutation to the presence of this disease.

RETINA X:1–13, 2011

Occult macular dystrophy (OMD) was first described by Miyake et al[1] to be a hereditary macular dystrophy without visible fundus abnormalities. Patients with OMD are characterized by a progressive decrease of visual acuity with normal-appearing fundus and normal fluorescein angiograms (FA). The important signs of OMD are normal full-field electroretinograms (ERGs) but abnormal focal macular ERGs and multifocal electroretinograms (mfERGs) also exist. These findings indicated that the retinal dysfunction was confined to the macula.[1–5] Optical coherence tomography (OCT) showed structural changes in the outer nuclear and photoreceptor layers.[6–11]

Recently, we found that dominant mutations in the *RP1L1* gene were responsible for OMD.[12] The *RP1L1* gene was originally cloned as a gene derived from common ancestors as a retinitis pigmentosa 1 (*RP1*) gene, which is responsible for 5–10% of autosomal dominant retinitis pigmentosa worldwide, on the same Chromosome 8.[13–17] A number of attempts have been made to identify mutations in *RP1L1* in various retinitis pigmentosa patients with no success. An immunohistochemical study on cynomolgus monkeys showed that *RP1L1* was expressed in rod and cone photoreceptors, and *RP1L1* is thought to play important roles in the morphogenesis of the photoreceptors.[13,18] Heterozygous *RP1L1* knockout mice were reported to be normal, whereas homozygous knockout mice develop subtle retinal degeneration.[18] However, the RP1L1 protein has a very low degree of overall sequence

From the *Laboratory of Visual Physiology, National Institute of Sensory Organs, Tokyo, Japan; †Division of Ophthalmology and Visual Science, Graduate School of Medical and Dental Sciences, Niigata University, Niigata, Japan; ‡Akiba Eye Clinic, Niigata, Japan; §Department of Ophthalmology, Sado General Hospital, Niigata, Japan; ¶Department of Ophthalmology, School of Medicine, Teikyo University, Tokyo, Japan; **Department of Ophthalmology, School of Medicine, Keio University, Tokyo, Japan; and ††Aichi Medical University, Aichi, Japan.

The authors have no financial interest or conflicts of interest.

Supported in part by research grants from the Ministry of Health, Labor and Welfare, Japan and Japan Society for the Promotion of Science, Japan.

Reprint requests: Kazushige Tsunoda, Laboratory of Visual Physiology, National Institute of Sensory Organs, 2-5-1 Higashigaoka, Meguro-ku, Tokyo 152-8902, Japan; e-mail: tsunodakazushige@kankakuki.go.jp

identity (39%) between humans and mice compared with the average values of sequence similarity observed between humans and mice proteins. The results of linkage studies have strongly supported the contribution of *RP1L1* mutations to the presence of this disease,[12] but the function of *RP1L1* in the human retina has not been completely determined.

A large number of cases of OMD have been reported[7,10,19]; however, we did not always find the same mutations in sporadic cases or in small families, which had less than three affected members. This led us to hypothesize that several independent mutations can lead to the phenotype of OMD, that is, OMD is not a single disease caused by a specific gene mutation, but may represent different diseases with similar retinal dysfunctions.

Thus, the aim of this study was to determine the characteristics of OMD by investigating the phenotypes of patients with the *RP1L1* mutation from a single Japanese family.

Patients and Methods

We investigated 19 members from a single Japanese family. A homozygous mutation, p.Arg45Trp in the *RP1L1* gene, was confirmed in 14 members,[12] and 13 of the 14 were diagnosed with OMD. Among the 14 members with a mutation in the *RP1L1* gene, 11 were followed-up at the Niigata University in Niigata, Japan. The other three were examined at the National Institute of Sensory Organs in Tokyo, Japan. Each member had a complete ophthalmic examination including best-corrected visual acuity (BCVA), refraction, perimetry, fundus photography, FA, full-field ERGs,[20] mfERGs,[21] and OCT. The visual fields were determined by Goldmann perimetry or by Humphrey Visual Field Analyzer (Model 750i; Carl Zeiss Meditec, Inc, Dublin, CA). The SITA Standard strategy was used with the 30-2 program or the 10-2 program for the Humphrey Visual Field Analyzer.

Electroretinograms were used to assess the retinal function under both scotopic and photopic conditions.[22] Full-field ERGs were recorded using the International Society of Clinical Electrophysiology and Vision standard protocol. Multifactorial electroretinograms were recorded with the Visual Evoked Response Imaging System (VERIS science 4.1; EDI, San Mateo, CA). A Burian–Allen bipolar contact lens electrode was used to record the mfERGs. The visual stimuli consisted of 61 or 103 hexagonal elements with an overall subtense of approximately 60°. The luminance of each hexagon was independently modulated between black (3.5 cd/m^2) and white (138.0 cd/m^2) according to a binary m-sequence at 75 Hz. The surround luminance was 70.8 cd/m^2.

The OCT images were obtained with a spectral-domain OCT (HD-OCT; Carl Zeiss Meditec or a 3D-OCT-1000, Mark II; Topcon) from 21 eyes of 12 cases in the same pedigree.

The procedures used adhered to the tenets of the Declaration of Helsinki and were approved by the Medical Ethics Committee of both the Niigata University and National Institute of Sensory Organs. An informed consent was received from all the subjects for the tests.

Results

The findings of 5 generations of 1 family with OMD are shown in Figure 1. The numbered family members had the same mutation in *RP1L1* (p.Arg45Trp), and family members designated with the filled squares or filled circles were phenotypically diagnosed with OMD by routine examinations including visual field tests, FA, mfERGs, and Fourier-domain OCT. Only Patient 5 (age 60 years) had normal phenotype, although she had the *RP1L1* mutation.

The clinical characteristics and the results of ocular examinations of all the 14 family members with the *RP1L1* mutation (p.Arg45Trp) are listed in Tables 1 and 2. Family Member #5 was diagnosed as normal because she had normal mfERGs.

Among the 13 OMD patients (average age at the final examination, 57.2 ± 22.1 years), 12 complained of disturbances of central vision and 4 complained of photophobia (Table 1). Patient 1 did not report any visual disturbances in the right eye as did Patient 6 for both eyes. The visual dysfunction in these eyes was confirmed by mfERGs. For 13 patients, the age at the onset of visual difficulties varied from 6 years to 50 years with a mean of 27.3 ± 15.1 years.

All the patients were affected in both eyes, and the onset was the same in the 2 eyes except for Patients 1, 11, 12, and 14. Patient 1 first noticed a decrease in her visual acuity in her left eye at age 50 years, and she still did not have any subjective visual disturbances in her right eye 30 years later. However, a clear decrease in the mfERGs in the macular area was detected in both eyes. Patient 11 first noticed a decrease in the visual acuity in her right eye at age 47 years when the BCVA was 0.2 in the right eye and 1.2 in the left eye (Figure 2). Seven years later at age 54 years, she noticed a decrease in the vision in her left eye. Similarly, Patients 12 and 14 did not report any visual disturbances in their right eyes until 2 (Patient 12) or 8 (Patient 14) years after the onset in their left eyes.

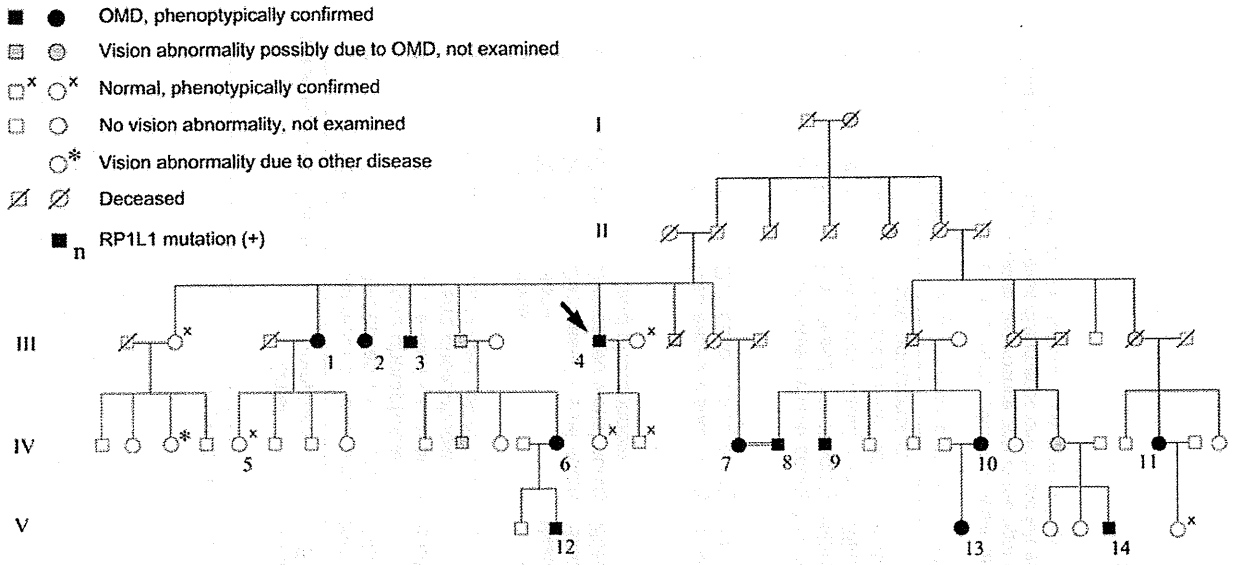

Fig. 1. Pedigree of a family with OMD. The identification number of the patients is marked beside the symbols. The proband is indicated by an arrow. The open squares and circles with crosses are the relatives whose visual function was confirmed to be normal by routine examinations including Humphrey visual field tests, mfERGs, and Fourier-domain OCT. Those designated by hatched squares or circles were reported to have poor vision with similar severity and onset as the other genetically confirmed OMD patients. One relative marked by an asterisk had unilateral optic atrophy because of retrobulbar neuritis.

The duration of the continuous decrease in the BCVA varied from 10 years to 30 years (mean, 15.6 ± 7.7 years) in 16 eyes of 9 adult patients. After this period, these patients reported that their vision did not decrease. Patients 2, 3, 8, and 14 complained of photophobia, and the degree of photophobia remained unchanged after the visual acuity stopped decreasing. Patients 1, 2, 4, 7, and 9 had additional disturbances of vision because of senile cataracts, and Patients 2 and 4 had bilateral cataract surgery. The visual disturbances because of the OMD were still progressing at the last examination in the left eye of Patient 11 (age 57 years), and both eyes of Patient 12 (age 20 years), Patient 13 (age 18 years), and Patient 14 (age 28 years).

Different systemic disorders were found in some of the patients; however, there did not seem to be a specific disorder, which was common to all of them (Table 1).

In the 16 eyes of 9 patients whose BCVA had stopped decreasing, the BCVA varied from 0.07 to 0.5 (Table 2). The BCVA of the left eye of Patient 6 was 0.07 because of an untreated senile cataract. If this eye is excluded, the final BCVAs of all the stationary eyes range from 0.1 to 0.5. Patient 2 had photophobia, and her BCVA measured by manually presenting Landolt rings on separate cards under room light was 0.4 in the right eye and 0.5 in the left eye, which was better than that measured by a Landolt chart of 0.3 in the right eye and 0.3 in the left eye with background illumination.

For the 13 patients whose original refractions were confirmed, 11 of 26 eyes were essentially emmetropic (<± 0.5 diopters). Both eyes of Patients 1, 3, 4, 6, and 8 and the left eye of Patient 5 were hyperopic (+0.675 to +4.625 diopters). The right eye of Patient 7, the left eye of Patient 12, and both eyes of Patient 13 were moderately myopic (–0.625 to –2.75 diopters). These results indicate that there is no specific refraction associated with OMD patients in this family.

The visual fields were determined by Goldmann perimetry or Humphrey Visual Field Analyzer. All the patients had a relative central scotoma in both eyes except for Patient 1 whose right eye was normal by Goldmann perimetry. In all cases, no other visual field abnormalities were detected during the entire course of the disease. In the patients examined shortly after the onset, a relative central scotoma was not detected by Goldman perimetry and was confirmed by static perimetry.

The fundus of all except one eye was normal. The left eye of Patient 9 had background diabetic retinopathy. At the first consultation at age 46 years, Patient 9 did not have diabetes, and the funduscopic examination and FA revealed no macular abnormalities. At the age 66 years, there were few microaneurysms in the left macula away from the fovea; however, OCT did not show any diabetic changes such as macular edema. The OMD was still the main cause of visual acuity reduction in this patient.

Six patients consented to FA, and no abnormality was detected in the entire posterior pole of the eye. It is noteworthy that both the fundus and FA of Patient 4 were normal at the age 73 years, which was >50 years

Table 1. Clinical Characteristics of the Family Members With RP1L1 Mutation (p.Arg45Trp)

Case	Age and Gender	Chief Complaint	Affected Eye	Age at Onset (Years)	Duration of Continuous Decrease in BCVA (Years)	Duration After the Onset (Years)	Systemic Disorders
1	81, F	Decreased visual acuity	Bilateral*	50	20	31	Hypertension
2	71, F	Decreased visual acuity and photophobia	Bilateral	25	25	46	Diabetes mellitus since 64 years of age
3	74, M	Decreased visual acuity and photophobia	Bilateral	30	10	44	Hyperlipidemia, angina pectoris
4	83, M	Decreased visual acuity	Bilateral	20	10	63	Hypertension, Multiple cerebral infarction at 73 years of age
5	60, F	None	—†	—	—	—	—
6	50, F	None	Bilateral*	Unknown	Unknown	Unknown	—
7	69, F	Decreased visual acuity	Bilateral	50	10	19	—
8	69, M	Decreased visual acuity and photophobia	Bilateral	28	10	41	Hypertension since 67 years of age, Surgery for ossification of the posterior longitudinal ligament at 45 years of age
9	66, M	Decreased visual acuity	Bilateral	30	15	36	Diabetes mellitus since 63 years of age
10	58, F	Decreased visual acuity	Bilateral	10	30	48	Rheumatoid arthritis since 46 years of age, Bronchiectasis since 43 years of age
11	57, F	Decreased visual acuity	Bilateral ‡	47	OD, 10, OS, still progressing	10	—
12	20, M	Decreased visual acuity	Bilateral§	14	Still progressing	6	Atopic dermatitis
13	18, F	Decreased visual acuity	Bilateral	6	Still progressing	12	—
14	28, M	Decreased visual acuity and photophobia	Bilateral¶	18	Still progressing	10	—

*Patient 1 has subjective visual disturbance only in the left eye, and Patient 6 does not have any subjective visual disturbances in both eyes. The visual dysfunction was confirmed by mfERG.

†This woman has a mutation in RP1L1, but her visual function was confirmed normal after routine examinations including mfERG.

‡This patient noticed visual disturbance only in the right eye at 47 years of age. The visual disturbance in the left eye was first noticed at 54 years of age.

§This patient noticed visual disturbance only in the left eye at 14 years of age. The visual disturbance in the right eye was first noticed at 16 years of age.

¶This patient noticed visual disturbance only in the left eye at 18 years of age. The visual disturbance in OD was first noticed at 26 years of age.

Table 2. Results of Ocular Examinations of the Family Members With RP1L1 Mutation

Case	Age and Gender	BCVA at Final Visit		Refraction (D)*		Visual Field	Fundus Appearance	FA	Full-Field ERG	Relative Amplitude in mfERG at Fovea (Ring 1/Ring 5 or Ring 6)†	Other Ocular Disorders
		OD	OS	OD	OS						
1	81, F	1.2	0.1	+4.25	+4.625	Relative central scotoma, OS	Normal, OU	Normal, OU	NE	2.34, OD, 0.60, OS	Senile cataract, OU
2	71, F	0.4	0.5	Unknown‡	Unknown‡	Relative central scotoma, OU	Normal, OU	NE	NE	Not measurable, OU	Cataract surgery, OS at 58 years of age, OD at 69 years of age, Ptosis, OU
3	74, M	0.2	0.3	+2.875	+3.375	Relative central scotoma, OU	Normal, OU	NE	NE	Not measurable, OU	Laser peripheral iridotomy, OU at 73 years of age
4	83, M	0.2	0.2	+1.0	+1.625	Relative central scotoma, OU	Normal, OU	Normal, OU	Normal ISCEV standard protocol ERG, OU	Not measurable, OU	Cataract surgery, OU at 80 years of age
5	60, F	1.2	1.2	−0.25	+0.875	Normal, OU	Normal, OU	NE	NE	4.24, OD, NE, OS	—
6	50, F	1.2	1.2	+1.0	+1.0	Relative central scotoma, OU	Normal, OU	NE	NE	2.74, OD, 2.23, OS	—
7	69, F	0.1§	0.07§	−0.625	+0.25	Relative central scotoma, OU	Normal, OU	NE	Normal ISCEV standard protocol ERG, OU	Not measurable, OU	Senile cataract, OU
8	69, M	0.1	0.1	+1.125	+0.675	Relative central scotoma, OU	Normal, OU	NE	Normal ISCEV standard protocol ERG, OU	1.01, OD, 1.30, OS	—